CHAPTER 7

NUMERICAL MODELING OF THE RHEOLOGICAL PROPERTIES OF LANDSLIDE GENERATED DEBRIS

7.1 Introduction

Slope failure results in dislodge of a specific quantity of earth material from its original position on the slope, which moves downslope owing to gravity. The dislodged geomaterial is known as debris. The movement of landslide generated debris is a complex phenomenon and are hazardous for infrastructures in the downslope areas due to their high speed and a large number of particles of varying size (few microns to large boulders). Delimiting the extent of endangered areas is fundamental to landslide risk assessment. These require accurate prediction of a landslide's runout behaviour (energy and velocity of flow) along with the spreading characteristic (runout distance, depth of the moving mass, damage corridor width, and depth of deposits once mobilised) (Hungr et al. 1999; Wong et al. 1997). Runout behaviour is a set of quantitative and qualitative spatially distributed parameters that define the destructive potential of a landslide. A realistic estimate of a landslide's runout behaviour depends on an adequate understanding of the generic factors that control the flow. Therefore, the effect of various physical and geotechnical properties of the slope on the rheology (flow behaviour) of the landslide generated debris have been studied. The landslide generated debris flow was modelled using the Distinct Element Method (DEM). A physical model was set up in the laboratory to calibrate the numerical simulation model. The calibrated numerical model with the desired level of reliability has been validated with a case study. After successful calibration and validation, parametric analysis was performed, which included the effect of slope angle, slope height, slope profile and particle size distribution of the debris on the flow behaviour. The effect of water content was studied by considering flow under

dry and wet conditions. The study of the effectiveness of remedial measures such as retaining walls/debris flow barrier was also performed.

7.2 Numerical Analysis Using Distinct Element Method

The DEM is based on Newton's law of motion and force-displacement law. It is beneficial in analysing granular material since it can effectively model large strain particle movement (non-continuum model) (Kruggel-Emden et al. 2007). DEM is a particle-based approach that essentially uses the first principle of physics that treats each particle of a granular bed individually. Each particle is represented through a representative shape and size that interacts with other particles and equipment geometry. These interactions are at the heart of the DEM implementation, and they are captured through different user-specified material properties. Multiple particle types with different properties (shape and size distribution, density, Young's Modulus, Poisson' ratio, cohesion, friction angle etc.), can be easily specified to capture the unique complexities of any system under investigation.

PFC (Particle Flow Code) is a general-purpose, distinct-element modelling framework developed by the ITASCA Consultancy group. It can model the synthetic materials composed of an assembly of variably-sized rigid particles that interact at contacts to represent both granular and solid materials (https://www.itascacg.com/software/pfc). PFC models simulate the independent movement (rotation and translation) and interaction of rigid particles that may interact at contacts based on the moment and an internal force. The present study has been performed using PFC since it can effectively model the dislodged geomaterial flow behaviour (debris). The basic unit in this method is a discrete particle, which can freely collide among itself and simultaneously interact with its surroundings.

Particle (geomaterial) movement can be grouped as free fall, bouncing, sliding and rolling. The loss of energy during collision is modelled with the help of mechanical damping (using spring and dashpot). A normal (βn) and shear (βs) dashpot represent viscous damping at particle contact are shown in Fig. 7.1. When there is contact between the two particles (1 and 2), their shear and normal stiffness is given by $K_s = (K_s1.K_s2)/ (K_s1+K_s2)$ and $K_n = (K_n1.K_n2)/ (K_n1+K_n2)$ respectively, and their directions are shown in Fig. 7.2 (https://www.itascacg.com/software/pfc). In DEM, mechanical parameters are not directly fed to the software. Since it calculates the model behaviour using the contact properties of the particle, various hit and trial attempts are performed to get macro-mechanical properties using different combinations of contact properties.

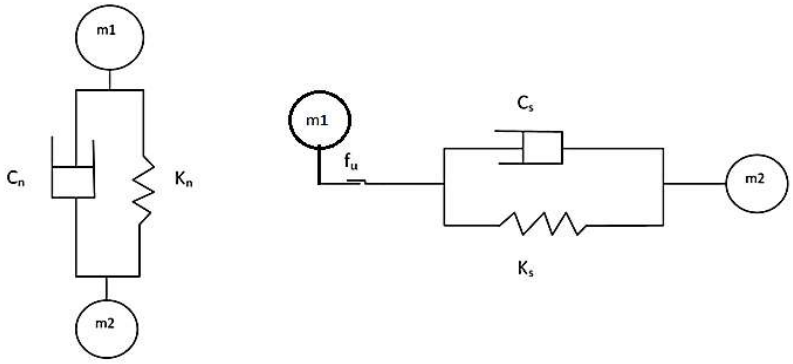

Fig. 7.1. Dashpot and spring representation for normal and shear viscous damping
(Source: https://www.itascacg.com/software/pfc)

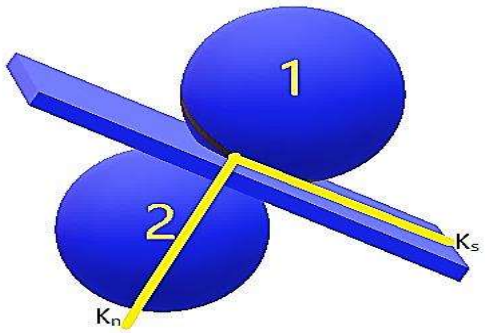

Fig. 7.2. Normal and shear stiffness with direction
(Source: https://www.itascacg.com/software/pfc)

The unique feature of DEM is that it can determine several flow parameters, including velocity, spread, energy and quantity of debris after failure. At the same time, other methods are only limited to failure conditions or type of failure (Poisel and Preh 2008). The method used for the present study is the Linear Model. The linear component provides linear elastic behaviour, while the dashpot provides viscous behaviour. Two linear springs provide normal (K_n) and shear (K_s) stiffness, whereas two dashpots provide normal (β_n) and shear (β_s) viscous force (https://www.itascacg.com/software/pfc).

7.3 Calibration of Numerical Model

A physical model was set up in the laboratory to calibrate particle's contact properties. The physical laboratory model consists of an artificial slope mimicking the natural conditions in scale down configurations. The artificial slope has been formulated into three layers with large rocks (10-15cm) are placed at the base of the slope mimicking the bedrock layer. Small size fractured rocks (3-6cm) mimicking the weathered rock layer are placed above the bedrock throughout the entire model, and the top layer placed above the weathered rock layer is made up of remoulded residual soil mimicking the top residual soil layer (Fig. 7.3). A remoulded residual soil mix having grain size distribution varying from 0.075mm to 20mm was used during laboratory physical model testing. The gradation for the residual soil mix includes 40% of the soil particle size ranges from 0.075mm to 0.425mm, 30% of the soil particle size ranges from 0.425mm to 2.0mm, 20% of the soil particle size ranges from 2.0mm to 4.75mm while the rest 10% of the soil particle size ranges from 4.75mm to 20mm. The slope inclination can be varied up to 60^0 with the help of a mechanical jack placed at the base of the model.

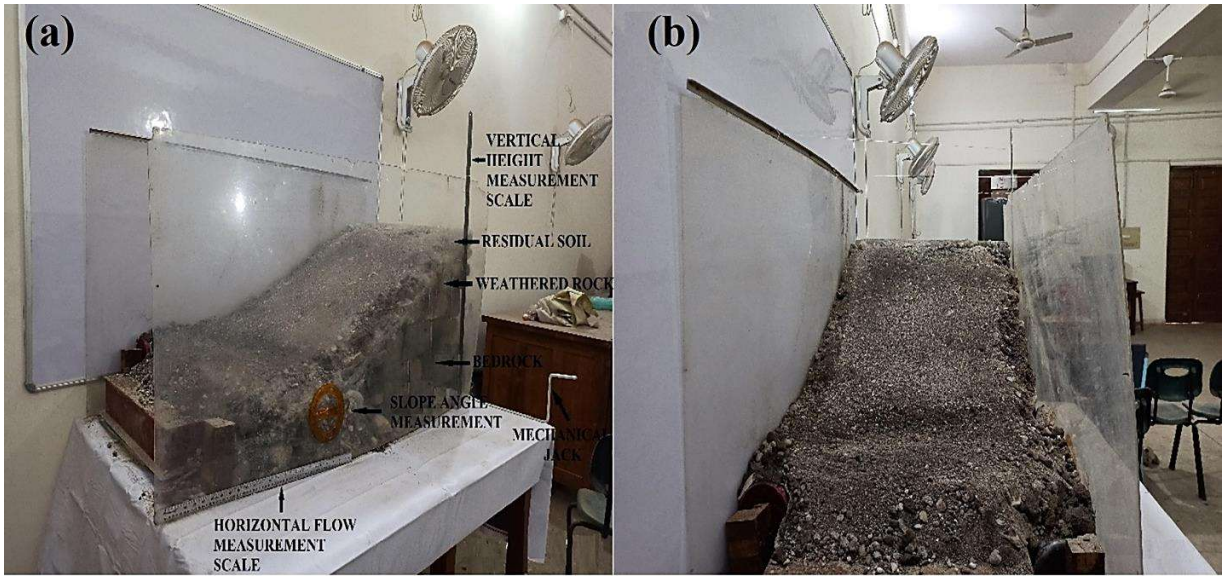

Fig. 7.3. The physical model developed in the laboratory for calibrating the numerical model (a) Side section and (b) Front section

The laboratory physical model test was numerically modelled using PFC (Fig. 7.4), where the individual particles were modelled in the form of Rblock. The Rblock template was created by importing 3-Dimensional geometry. The various shapes of Rblock templates used in the current study are shown in Fig. 7.5. Multiple numerical models were made with different contact properties to simulate the physical model (laboratory model) result. Contact properties used in the numerical simulation were determined by the hit and trial method. The grain size distribution of the top residual soil layer was varied from 1mm to 20mm in the developed numerical model using PFC. Very fine particles (<1mm) were left out during simulation since they do not affect the interparticle collision forces between the flowing debris to a much extent, and choosing finer particles will unnecessarily increase the computational time (Ding et al. 2014; Xu et al. 2020). However, the smaller particle does affect the contact properties of Rblock-Rblock interaction during landslide debris flow, which was obtained by calibrating the numerical model with the laboratory test results and is implemented in the final numerical simulation model.

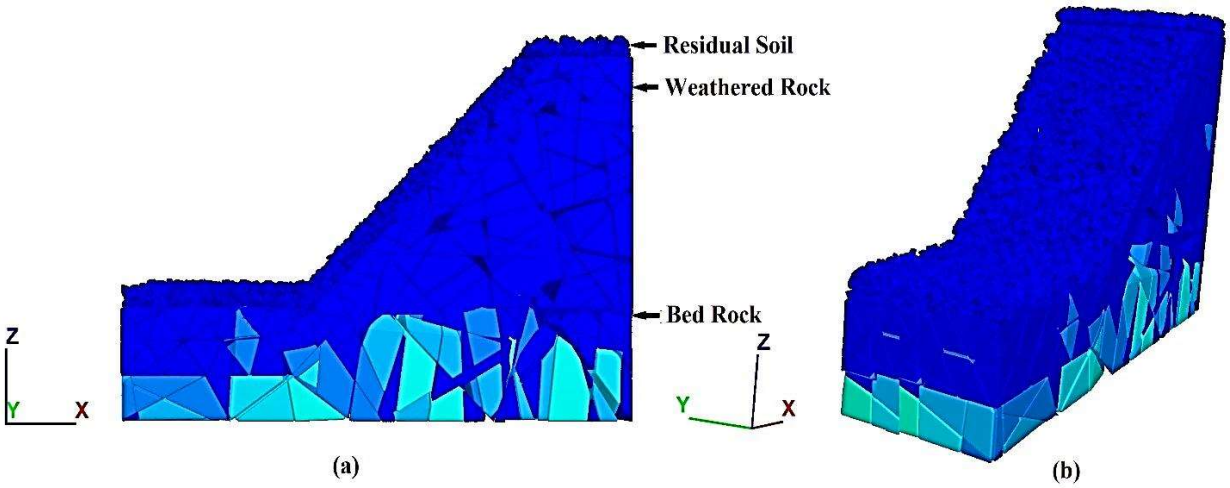

Fig. 7.4. Numerical model corresponding to the physical laboratory model (a) Side section and (b) Front section

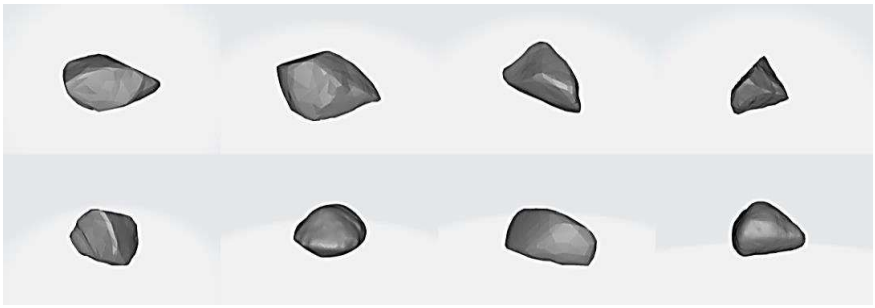

Fig. 7.5. Various Rblock templates used during numerical simulation

Total four physical models have been tested at slope angle 45^0 and 50^0 (two for dry condition and two for wet condition) in the laboratory. The physical model tests result has been used for calibrating the numerical model using PFC. The failure and debris flow pattern during laboratory testing under the dry condition with the corresponding numerical model developed in PFC are shown in Fig. 7.6. The detailed comparison results of a 60cm high laboratory slope model having an inclination of 45^0 and 50^0 under a dry and wet condition with that of the corresponding numerical model in PFC are given in Table 7.1. The final contact properties obtained after calibrating the developed numerical model is given in Table 7.2. The contact properties obtained

from calibration will be used for validating a case study and further during parametric analysis to obtain the debris flow behaviour.

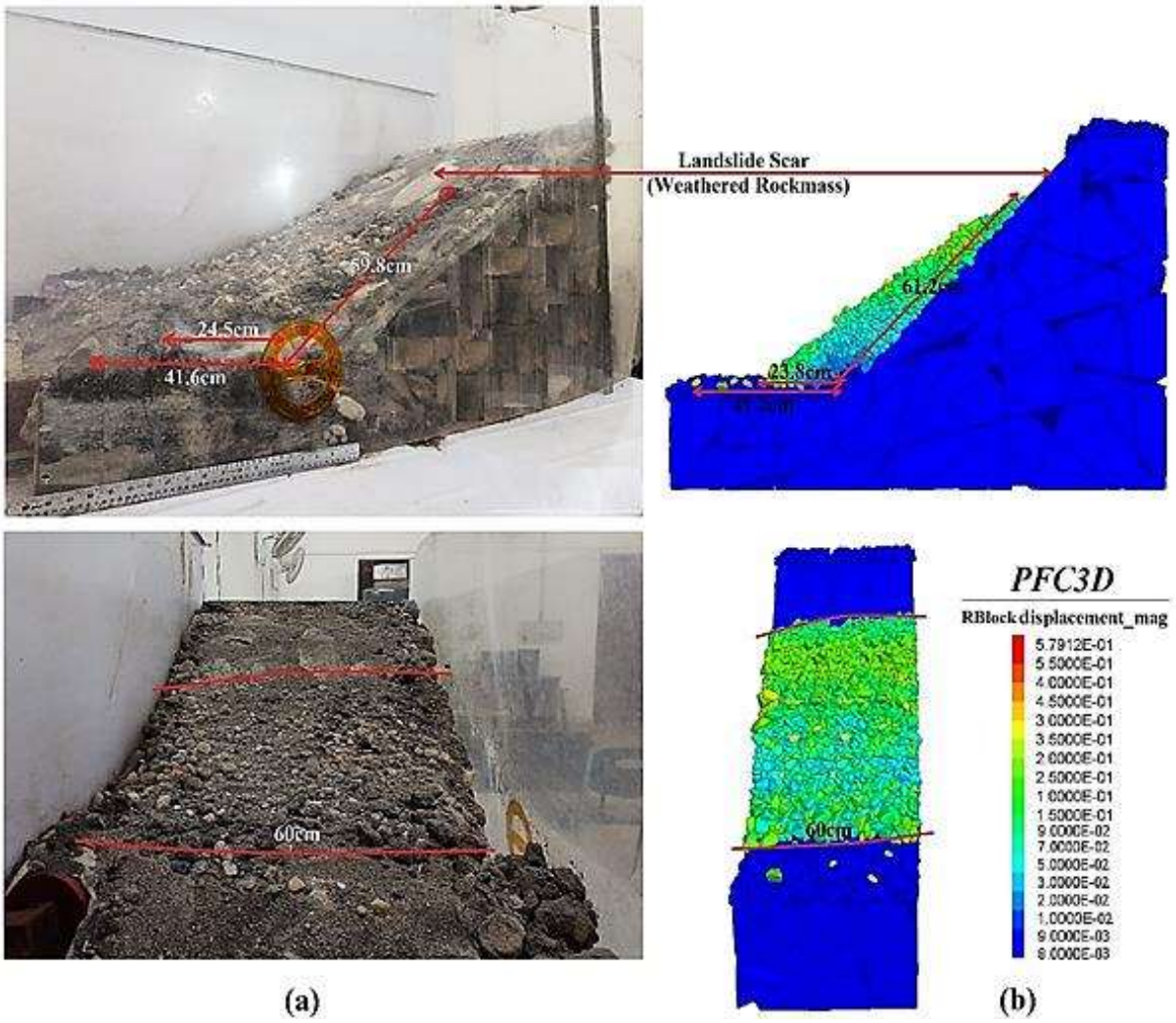

Fig. 7.6. Landslide debris flow comparison study for a 60cm high and 45^0 dry slope (a) physical model and (b) numerical simulation

Table 7.1: Comparison between physical testing (Laboratory) and numerical model (PFC) result for a 60cm heigh slope

Parameter	Dry Condition (0% WC or 0% Saturation)				Wet Condition (30% WC or 100% Saturation)			
	45^0 Slope Inclination		50^0 Slope Inclination		45^0 Slope Inclination		50^0 Slope Inclination	
	Lab Model	Numerical Model	Lab Model	Numerical Model	Lab Model	Numerical Model	Lab Model	Numerical Model
Maximum distance travel from toe (cm)	41.6	41.2	46.5	45.9	49.1	49.8	55.3	54.8
Spread along strike line at toe (cm)	60	60	60	60	60	58.6	60	60
Average particle spread at toe (cm)	24.5	23.8	26.6	26.1	27.3	27.9	30.5	29.7
Length of particle settlement along the slope (cm)	59.8	61.2	52.3	51.2	42.5	41.3	36.7	35.6
Minimum time taken by debris to reach the toe (sec)	0.45	0.48	0.37	0.33	0.32	0.35	0.31	0.29
Time taken for complete settlement of debris (sec)	1.07	1.10	0.96	0.92	0.86	0.91	0.79	0.75
Settlement description	Larger particles travelled more than smaller ones. Smaller particles settled at the bottom below the larger ones.	Larger particles travelled more than smaller ones. Smaller particles settled at the bottom below the larger ones.	Larger particles travelled more than smaller ones. Smaller particles settled at the bottom below the larger ones.	Larger particles travelled more than smaller ones. Smaller particles settled at the bottom below the larger ones.	Larger particles travelled more than smaller ones. Smaller particles settled at the bottom below the larger ones. Spread is more compared to dry flow.	Larger particles travelled more than smaller ones. Smaller particles settled at the bottom below the larger ones. Spread is more compared to dry flow.	Larger particles travelled more than smaller ones. Smaller particles settled at the bottom below the larger ones. Spread is more compared to dry flow.	Larger particles travelled more than smaller ones. Smaller particles settled at the bottom below the larger ones. Spread is more compared to dry flow.

Table 7.2: Contact properties obtained from calibrating the numerical model with the laboratory test model

Attribute	Dry	If modified (during fall)	Wet	If modified (during fall)
Method	Linear	-	Linear	-
Effective modulus	1.20E+08	-	1.20E+08	-
Normal-to-shear stiffness ratio	2.3	-	2.3	-
Friction coefficient	0.6	0.6	0.32	0.35
Normal critical damping ratio	0.56	0.6	0.41	0.45
Dashpot mode	No-tension normal & full shear	-	No-tension normal & full shear	-
Normal-force update mode	Incremental Update	-	Incremental Update	-
Density	2700	-	2700	-
Local Damping coefficient	0.4	0.4	0.29	0.30

7.4 Validation of Numerical Model

After calibrating the contact properties for the developed numerical model by using the results of the physical laboratory model, a case study of the Varunavat landslide was taken to validate the developed numerical model. Varunavat hill is situated in Uttarkashi (78°26’ E 30°44’ N) at the bank of the sacred river Bhagirathi. A series of landslide events occurred during the monsoon season of 2003, which rendered heavy loss of infrastructure Fig. 7.7 (Nawani et al. 2015; Parkash 2011). The toe of the hill is at an elevation of 1100m, and the top is at 1840m from Mean Sea Level (MSL) (Sai et al. 2008). Geologically this area is characterised as Higher Himalayan crystalline and Lesser Himalayan sediments with 1-2m thick soil cover (Sarkar et al. 2011). The upper portion of the hill (above 1670m from MSL) is loose, unconsolidated, overburdened mass with gentle topography, while the portion below 1670m from MSL constitute a rocky slope. Between 1640m to 1530m above MSL, it has a thick pile of old and fresh debris slide (Nawani et

al. 2015). About 40000-50000m^3 of debris was displaced during the landslide (Sarkar et al. 2011). The dislodged debris rolled down through three transportation chute tracts:

i. Tambakhani chute

ii. Masjid mohalla chute

iii. Ram Lila ground

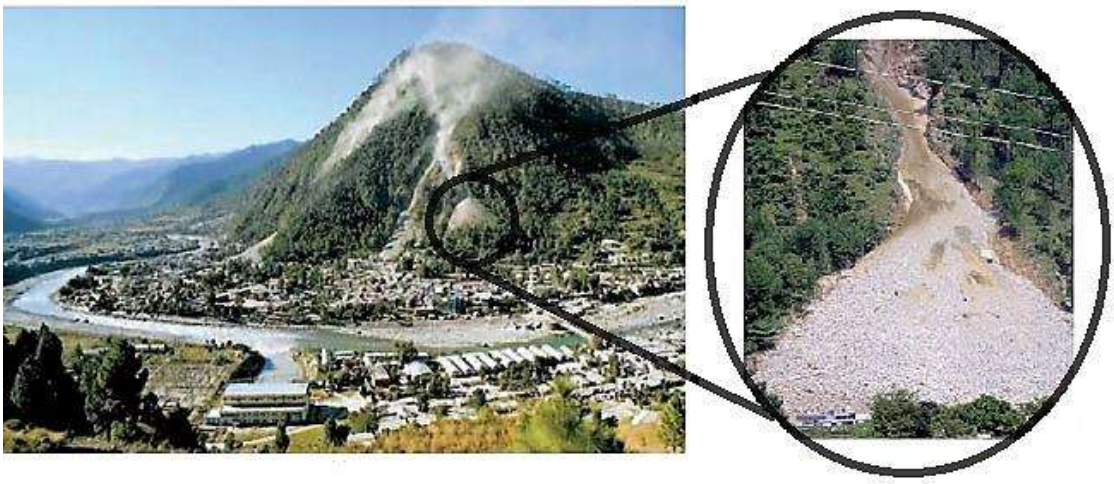

Fig. 7.7. Slope failure and debris flow in Varunavat Hill, September 2003 (Sarkar et al. 2011)

The Varunavat landslide is modelled with PFC using rblock and wall features. The coordinate of the Masjid Mohalla slide was 78°26'20.1'' E and 30°44'09.6'' N, and the coordinates of the Tambakhani chute were 78°26'17.7'' E and 30°44'10.4'' N (Pande and Uniyal 2007). Masjid Mohalla slide was spitted into two parts one was Masjid mohalla chute, and another was Ramlila ground chute. Various field parameters obtained from a detailed investigation of the landslide by several researchers are given in Table 7.3.

Table 7.3: Salient features of Varunavat landslide

Source	Start of Slide (above MSL)	Crown (above MSL)	Length	Width(widest)	Width(shortest)	Debris volume
Sai et al. (2008)	1400-1500m	-	650m	100m(middle)	5-10m	-
Kumar et al. (2003)	below 1670 m	1670-1704m	620m	120m(middle)	-	-

Sarkar et al. (2011)	-	-	700m	60m	6m(bottom)	40,000-50,000m^3
Pande and Uniyal (2007)	-	-	700m	60m	5m(toe)	-
Nawani et al. (2015)	-	1670-1800m	-	-	-	-

The geometry of the Varunavat hill area was downloaded in the form of Digital Elevation Data of 30m resolution available from open source CARTOSAT data at Indian Geo-Platform BHUVAN (https://bhuvan.nrsc.gov.in). After downloading the data, the '.stl' file was generated for the area between coordinates (30.720^{0}N, 78.425^{0}E) and (30.740^{0}N, 78.445^{0}E), where the coordinate represents two ends of a diagonal. The approximate length of the square area was around 2210m, and the scale used to model the geometry in PFC was 1 unit = 4m. The highest and lowest points in the selected geometry domain were at an elevation of 1839m and 1053m, respectively, which is in accordance with Nawani et al. (2015). The '.stl' file was imported in PFC to generate a wall. Fig. 7.8 depicts the topography of the site obtained through Digital Elevation Data and corresponding walls generated in PFC.

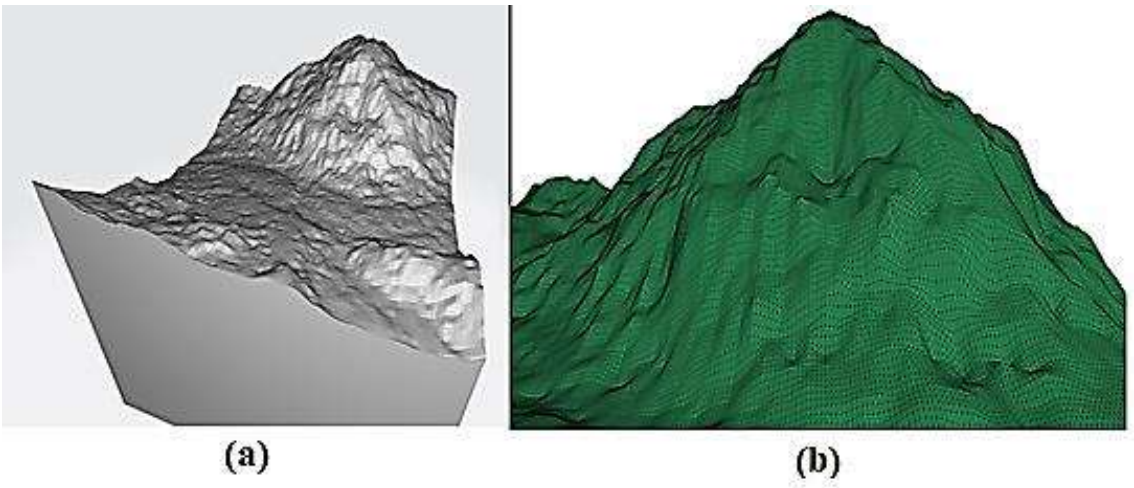

Fig. 7.8. Topography of Varunavat Hill (a) Digital elevation model (b) Wall generated in PFC

Around 80,000 rblock have been generated with sizes ranging from 1mm to 5000mm, where 60% particles were in the range 1mm to 50mm, 20% were between 50mm to 1000mm, 15% were between 1000mm to 3000mm and rest 5% particles range between 3000mm to 5000mm. The gradation of the landslide generated debris has been chosen based on detailed investigations performed by Sarkar et al. (2011), Nawani et al. (2015) and Parkash (2011). The maximum boulder size observed in the landslide was around 4-6m in diameter (Sai et al. 2008). Thus, in the current study, the maximum size of the particles was limited to 5m. The weathering grade of the site was W1-W3, i.e., with joint spacing between 1cm to 100cm (Kumar et al. 2003). Very fine particles (<1mm) were left out during simulation since they do not affect the interparticle collision forces between the flowing debris to a much extent, and choosing finer particles will unnecessarily increase the computational time (Ding et al. 2014; Xu et al. 2020). However, the smaller particle does affect the contact properties during landslide debris flow, which is modelled by taking the proper contact properties for Rblock-Rblock and Rblock-Facet, as obtained through calibration of the developed numerical model using laboratory physical model as given in Table 7.2.

Rblocks were first settled in a box at the crown of the landslide then were allowed to flow under gravity by deleting the box. During the settlement of the rblocks (or before flow initiation), the natural weathering process (i.e., weathering decreases with depth) was mimicked by placing the larger particles at the bottom while the smaller ones at the top (Ray et al. 2020a). The total flow length in the model was observed to be around 671.62m, while the broadest length of the landslide was 106.2m at the middle of the slide, and the shortest was less than 11m at the toe. Some of the larger particles with a size of more than 3m spread over a considerable distance. The various instances of flowing debris at different time frames are shown in Fig. 7.9. The results

obtained during numerical simulation are compared with the actual site data (Table 7.3) and are within good approximation to the Varunavat Hill landslide, as shown in Table 7.4.

Table 7.4: Comparison between actual parameters and modelled output

Parameter	**Actual Observation**	**Model Outcome**
Length of flow	650-700m	671.62m
Widest	120m	106.2m
Shortest	6m	11m
Spread (middle)	60-120m	68.7-113.4m
Pattern of flow	Split into two-part	Split into two-part

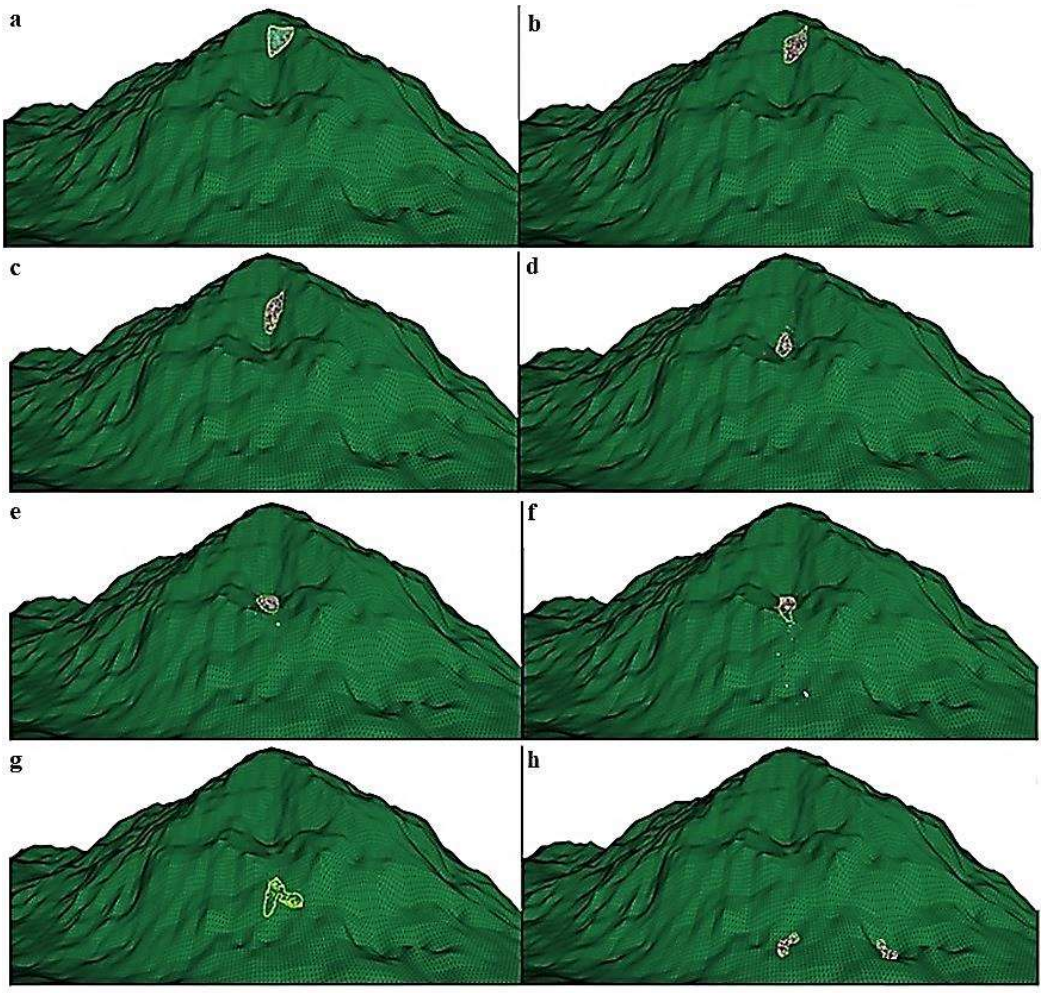

Fig. 7.9. The flow of debris over Varunavat Hill at a different time frame

Based on these results, it can be concluded that PFC can model landslide debris flow with an acceptable confidence level. It is also evident by comparing the result of the case study, and numerical verification model that changes in contact properties with size was negligible. The numerical model can simulate the size effect with good approximation. It also shows the broad applicability of numerical simulation, which saves time and resources while allowing precise calculation of various rheological properties of landslide debris without setting up large physical models with high reliability.

7.5 Parametric Analysis

An attempt has been made to simulate the effect of topographical and geotechnical variation of the slope in the rheological properties of landslide generated debris using PFC. It includes variation in slope height, slope angle, slope profile and particle size distribution of the dislodged slope mass under dry (0%WC) and wet (30%WC) conditions. Slope height is varied from 20m to 100m (at an interval of 20m), and slope angle is varied from 15^0 to 75^0 (at an interval of 15^0). The slope profile is modelled with three different curvatures, namely concave, flat and convex profile. The same slope profile along with its stratigraphy as illustrated in Fig. 7.4 was used for the parametric study. However, the height of the slope has been varied from 20m to 100m compared to the laboratory model, where the maximum height was limited to 1m. Therefore, the particle size range for the three layers has been changed and updated. For parametric analysis, the size range of the bedrock blocks was varied from 7-10m and were placed throughout the base of the slope. Above the bedrock, small fractured rocks of size ranging from 2-5m mimicking the weathered rock layer are placed throughout the entire model, and the top layer above the weathered rock layer is made up of residual soil. The depth of the residual soil layer was kept around 3-5m with particle gradation given in Table 7.5, while the depth of the weathered layer was around 5-

10m. The rest depth was filled up with bedrock. The effect of smaller particles of the residual soil layer is taken care of by using the contact properties (Table 7.2) obtained after calibration of the developed numerical model.

Table 7.5: Particle size distribution of the debris used during numerical simulation

Size (mm)	Fraction
1-50	0.45
50-200	0.35
200-500	0.15
500-1000	0.05

Several flow parameters of the debris, which includes the maximum and average distance travelled by debris from the toe of the slope in the direction of the valley, the average magnitude of the velocity and kinetic energy per unit volume, has been recorded. These parameters were also recorded for the four different size ranges of particles present in the residual soil (Table 7.5**).** These parameters give a good insight into collision and momentum transfer between the particles. Apart from this, the qualitative analysis of flow was also observed.

Finally, the effect of the retaining wall/debris flow barrier has also been studied. The different position of the wall along the slope surface has been varied from toe to upslope position on the slope. Two additional parameters have been measured along with flow parameters for the retaining wall's model. The first one is the fraction of total debris retained by the wall, along with the fraction retained for individual particle group size. The other one is the force and moment of the force due to the impact of the moving debris on the wall. It will prove beneficial in deciding the type and structural strength of the selected retaining wall/debris flow barrier.

7.5.1 General Observations

The debris flow is a complex phenomenon involving the transfer of momentum through collision and loss of energy due to inelastic collision, air and water (if present), resistance and

friction etc. After collision and separation of landslide-debris particles during the flow, apparent sorting phenomena were observed during the accumulation process. Finer particles are widely distributed near the toe of the slope and bottom of the deposit, while the coarser particles are widely distributed in the front and surface of the deposit (Fig. 7.10a). This can lead to a severe problem, as seen in many landslide incidences where the larger size boulders have travelled to a considerable distance in the valley and destroying/damaging engineered structures on their path. The smaller particles undergo more collisions compared to larger particles. As a result, smaller particle loses most of their energy due to frequent collision, whereas lesser collision in larger particles results in less energy dissipation. So, smaller particles spread over a limited area, whereas larger particles can spread up to a considerable distance causing damage to a larger area.

It was also observed that the average maximum distance travelled by debris is much greater in the case of the wet slope than the dry slope (Fig. 7.10b). The presence of water in the debris reduces the damping between inter-particle collision; thus, lesser dissipation of kinetic energy of the flowing debris takes place. Also, presence of water reduces the interparticle frictional force, allowing greater displacement of wet debris compared to dry one. The average distance reached by different particle size ranges of the debris displays an almost uniform range (16.26m to 17.72m) in the case of wet debris flow. However, the sorting effect occurs in the case of dry debris flow, where a limited average distance is reached by finer particles (up to 4.79m) from the toe. In contrast, a much longer average distance (up to 13.25m) is reached by the larger boulders. In dry condition, the average particles spread (4.79m to 13.25m) of the entire debris is more compared to wet condition (16.26 to 17.72m); however, the average distance of spread of the entire debris as well as the maximum distance travelled by a debris particle is more under the wet condition as noted in Table 7.6.

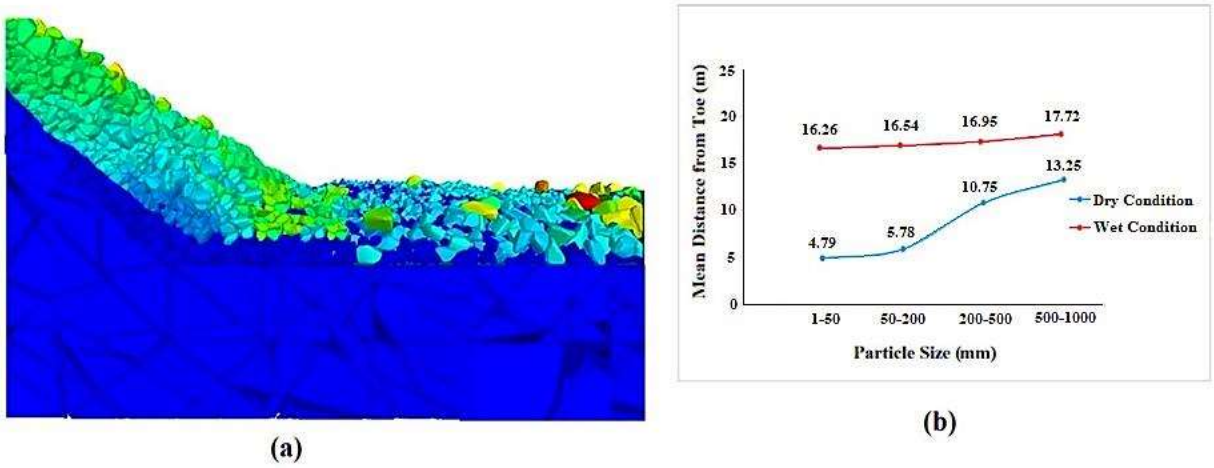

Fig. 7.10. For a 40m high slope with an inclination of 45^0 (a) Final settlement and distribution profile of the debris (b) Spread of different size particles

Table 7.6: Distance of debris spread from toe for the entire debris volume

Dry Debris		**Wet Debris**	
Mean (m)	4.94	Mean (m)	16.38
Variance	3.54	Variance	0.116
Max (m)	29.03	Max (m)	38.58

7.5.2 Effect of Slope Height

Five models having a constant slope angle of 45^0 and a varying slope height of 20m, 40m, 60m, 80m and 100m were created using PFC for each dry and wet condition. With an increase in the height of the slope, potential energy increases, which converts to kinetic energy during the downslope movement of debris. This behaviour is shown in Fig. 7.11, where kinetic energy per unit volume of particles increases with an increase in the height of the slope. It is evident that with a five times increase in slope height (20m to 100m), there is almost 4 and 3.5 times increase in kinetic energy per unit volume in case of wet and dry debris, respectively. The variation in kinetic energy per unit volume of the flowing debris in case of wet and dry debris is not profound in short height slope (20m); however, as the height increases, significant difference kinetic energy per unit

volume in case of wet and dry debris is observed for a particular slope height. Time taken to attain the peak kinetic energy per unit volume is lesser in wet debris as compared to dry debris.

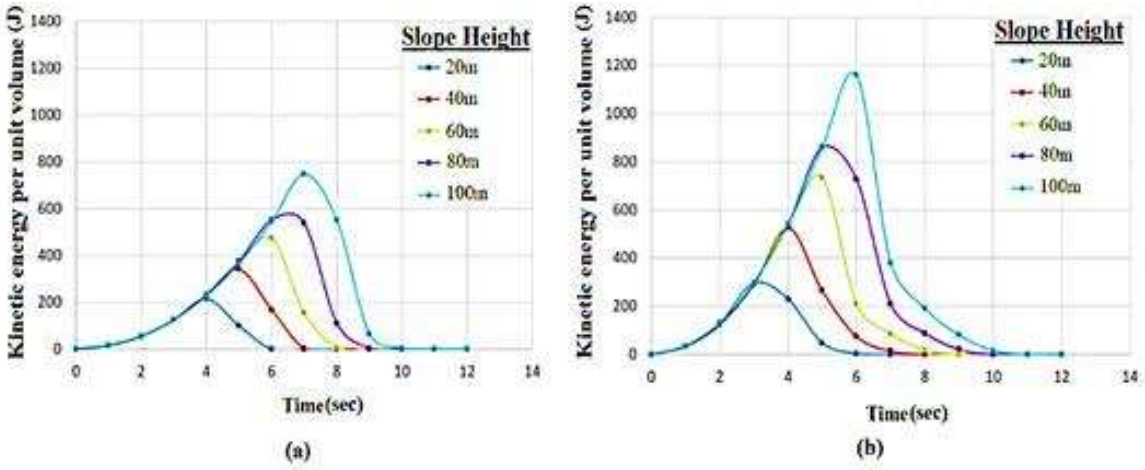

Fig. 7.11. Variation of kinetic energy per unit volume of the entire (a) Dry debris and (b) Wet debris with time for a 45^0 slope with a varying slope height

Thus, the height of the slope significantly affects the energy of the flowing debris. This energy is responsible for the spread of debris in the valley. The higher the slope, the higher the kinetic energy per unit volume, resulting in a relatively large displacement of the particle in the valley and vice-versa. This is demonstrated in Fig. 7.12a, where a nearly perfect linear relationship is obtained for a mean distance (X_{mean}) travelled by entire debris from toe in the direction of valley and height of slope (H). The X_{mean} in the case of wet debris is almost double compared to dry debris. This is owing to the higher kinetic energy per unit volume of the wet debris in comparison to the dry debris, as noted in Fig 7.11. However, when the individual particle size of the debris is considered, there is a marked variation between the average displacement of different size particles from the toe v/s height of the slope.

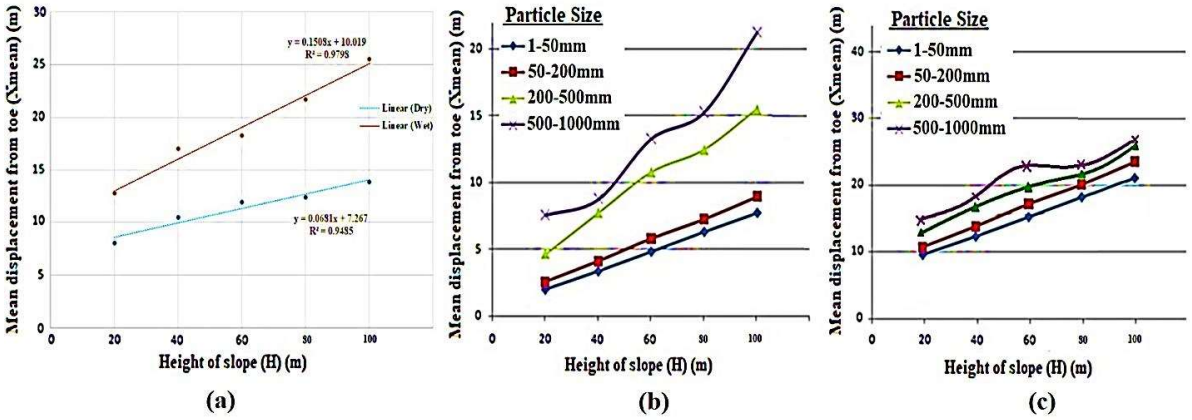

Fig. 7.12. Average distance travelled by (a) entire debris (b) individual particle groups in dry debris, and (c) individual particle groups in wet debris from toe v/s height of the slope for a 45^0 slope

It was observed that smaller particles show almost linear behaviour, whereas large particle shows a non-linearly trend (Fig. 7.12b,c). This may be attributed to the fact that with the increase in particle size (mass), a substantial variation in momentum is observed after inter collision between particles resulting in the non-linear flow pattern. Also, since the smaller particle (<200mm) dominates the debris material (80%) in the current study, almost linear variation between the mean displacement of particles from toe (X_{mean}) and height of slope (H) is observed for the whole debris flow (Fig. 7.12a) which may not be the case if the fraction of larger size particle increases in the flowing debris. So, it can be inferred that randomness in the spread of debris increases if larger particles are significant in fraction. Also, it must be noted that the presence of water in the debris brings more uniformity to flow for different particle sizes, as observed in the case of Dry and Wet flow (Fig. 7.12b, c). The variation between maximum distance travel by different size particles of the debris remains almost constant for different slope heights in the case of wet flow. In contrast, a marked variation in maximum distance travel by different size particles of debris exists in the case of dry flow with variation in slope height.

The graph between kinetic energy per unit volume and time of flow for particles of different size ranges shows a sharper peak for larger size particles. In contrast, a relatively flat peak was observed in the case of smaller size particles under both dry (Fig. 7.13) and wet (Fig. 7.14) debris flow. Also, the kinetic energy per unit volume with the flow for particles of different size range under wet conditions is much higher compared with flow under dry condition. The time taken to reach the peak kinetic energy per unit volume by the particle of the different size range of the debris is lesser in the case of the wet slope than the dry slope for all slope heights.

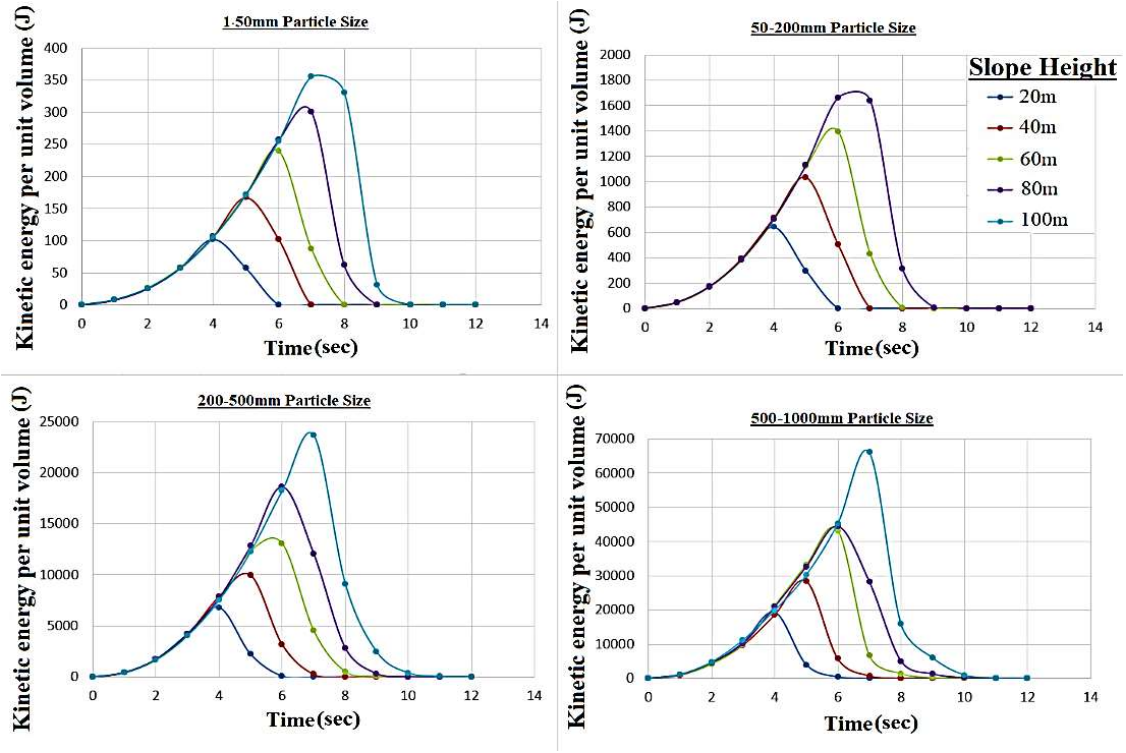

Fig. 7.13. Variation of kinetic energy per unit volume with time for a 45^0 slope with varying slope height for different particle size range under dry flow

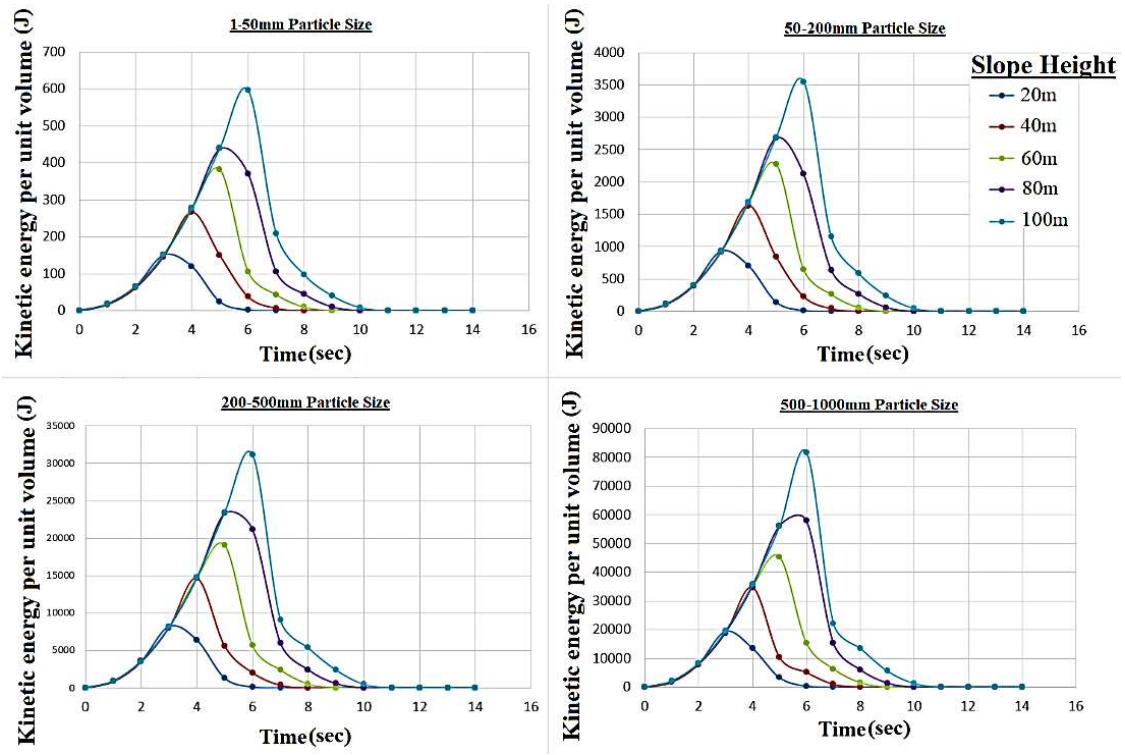

Fig. 7.14. Variation of kinetic energy per unit volume with time for a 45^0 slope with varying slope height for different particle size range under wet flow

For a 40m high slope with an inclination of 45^0, the variation of the average kinetic energy and velocity for different size groups of particles with time is given in Fig. 7.15 and Fig. 7.16, respectively, for both wet and dry debris flow. It is evident from the kinetic energy and velocity distribution graph that the magnitude of the average kinetic energy and velocity of large particles was higher compared to small particles for a particular slope height and inclination. It was observed that the peak average kinetic energy of the larger size particles (500-1000mm) is almost the same for both dry and wet flow. However, the peak average kinetic energy of the smaller size particle (<500mm) is more in the case of wet debris flow than corresponding dry debris flow.

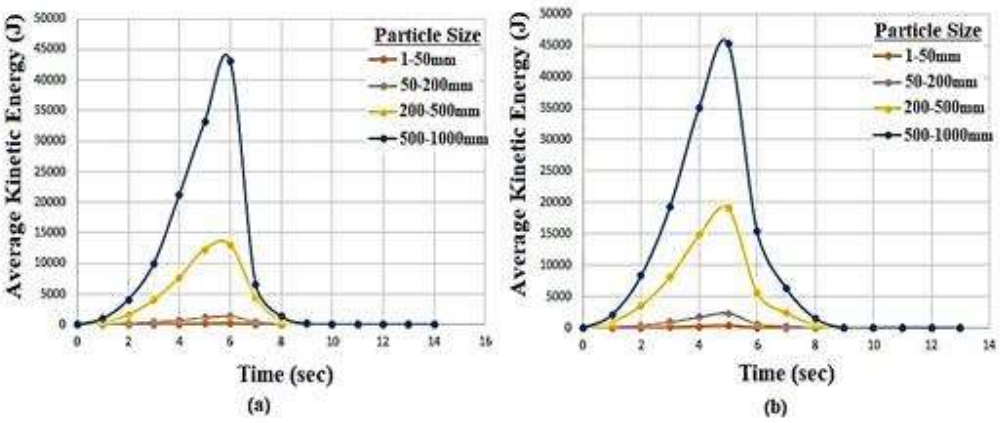

Fig. 7.15. Variation of the average kinetic energy of debris with time for individual particle size range for (a) dry and (b) wet debris for a 40m high slope with an inclination of 45^0

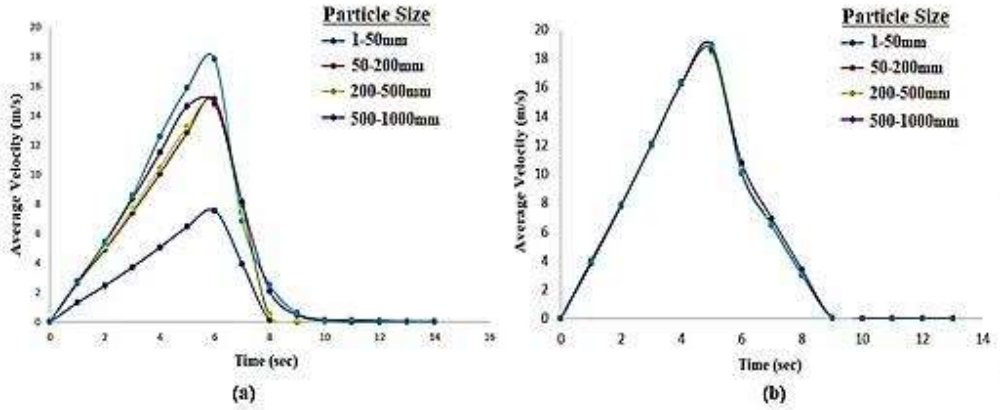

Fig. 7.16. Variation of the average velocity of debris with time for individual particle size range for (a) dry and (b) wet debris for a 40m high slope with an inclination of 45^0

In the case of peak average velocity attained by particles of different sizes, there is a marked variation in the case of dry debris flow where the velocity of the particles decreases with size and the larger particle (500-1000mm) is almost three times faster that of the smaller ones (1-50mm). However, in the case of wet debris flow, the average velocity of all the particle classes shows an almost similar range. The maximum average velocity attained by all the particle ranges of wet debris flow is almost equal to that of the larger particle (500-1000mm) during dry debris flow. Thus, in the case of dry debris flow, the large size boulders with high kinetic energy and velocity

are expected to cause most of the destruction to life and infrastructure during a landslide. In the case of wet debris flow, particles of all size ranges will have the almost same velocity of flow; however, the kinetic energy of the flowing debris will depend on the debris composition. The maximum destruction will be caused by debris composed of mainly large boulders flowing under wet conditions.

7.5.3 Effect of Slope Angle

Five models having a constant slope height of 40m and a varying slope angle of 15^0, 30^0, 45^0, 60^0 and 75^0 were created using PFC for each dry and wet condition. The model with a 15^0 slope angle did not show any considerable flow of particles; thus, it can be deduced that the 15^0 slope was insufficient for particles to flow. For remaining slope inclinations, the mean distance travelled by debris from toe (X_{mean}) shows the maximum value for 45^0 slope angle, as shown in Fig. 7.17. For gentle slopes ($<40^0$), most of the energy of the flowing debris gets dissipated during flow due to the considerable distance it has to cover till it reaches the toe. Whereas, for steep slopes ($>60^0$), although the particle has maximum energy, it gets quickly dissipated due to collision as soon as the direction of the flow path changes from slope face to horizontal surface as it reaches the toe. Moderate inclinations (40^0-50^0) provide the optimum energy and resultant flow direction resulting in a maximum reach of particles. In fact, particles of all size range show maximum distance travel at 45^0, which is evident from Fig. 7.18. For all the cases of slope inclinations, the spread of debris under wet conditions is almost 2-3 times more than the corresponding debris under dry conditions.

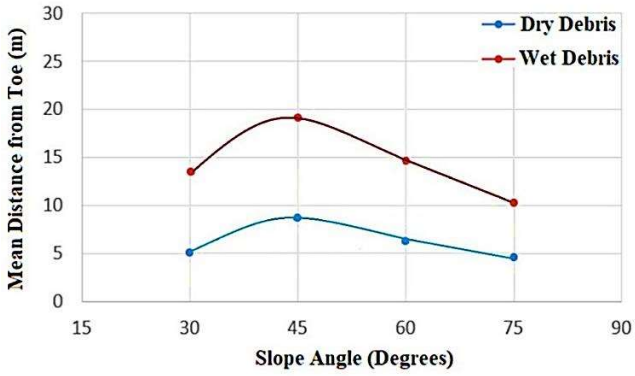

Fig. 7.17 Variation of average distance travelled by debris from toe v/s slope angle for a 40m high slope

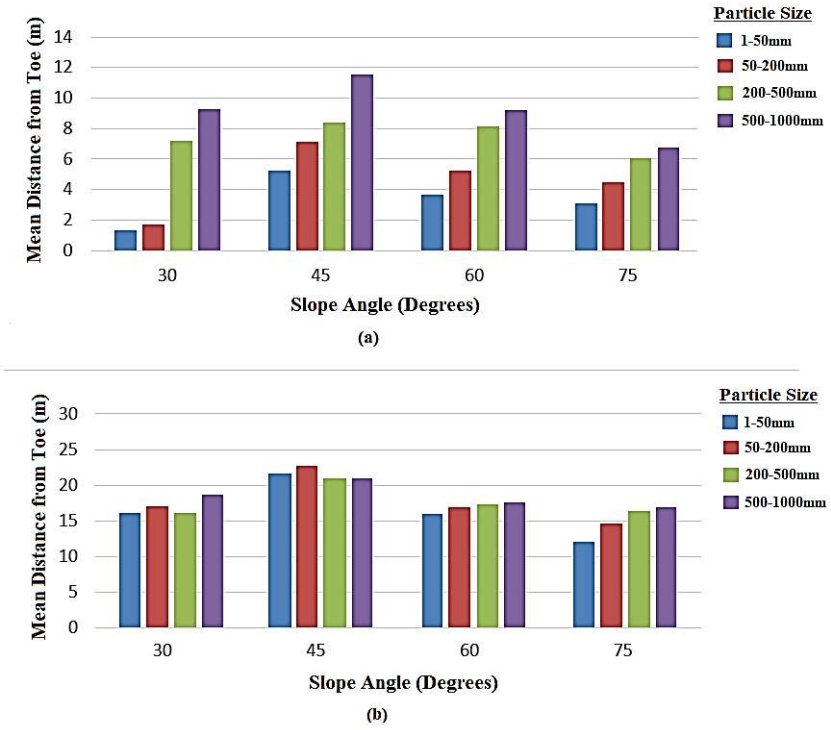

Fig. 7.18 Variation of average distance travelled by particles of different size groups under (a) Dry and (b) Wet conditions from the toe for different slope angles for a 40m high slope

With an increase in slope inclination, the average kinetic energy of debris increases while time to reach toe decreases and vice-versa (Fig. 7.19). This is valid for both dry and wet debris flow. However, the average kinetic energy of the wet debris is always greater than the

corresponding dry debris for any particular slope inclination. Increasing the slope inclination from gentle to steep resulted in an increase in 2.5 times the average kinetic energy for wet debris and 5:9 for dry debris flow. Fig. 7.20 depicts the velocity variation of the flowing debris with time for different slope inclinations. A constant increase in the average velocity of debris flow is observed with an increase in the slope inclinations. However, the average velocity of the wet debris is always greater than the corresponding dry debris for any particular slope inclination. With an increase in slope inclination from gentle to steep (i.e., 30^0 to 60^0), the average velocity of the flowing debris increases by 2.8 and 4.4 times under wet and dry conditions, respectively. From Fig. 17 and Fig. 18, it can be concluded that slope failure in the case of the gentle ($<40^0$) and steep ($>60^0$) slope will result in more localised damages near the toe area in the valley whereas, failure in moderate (40^0-50^0) slopes will result in more widespread damage in the valley, as seen in many past events in the study area.

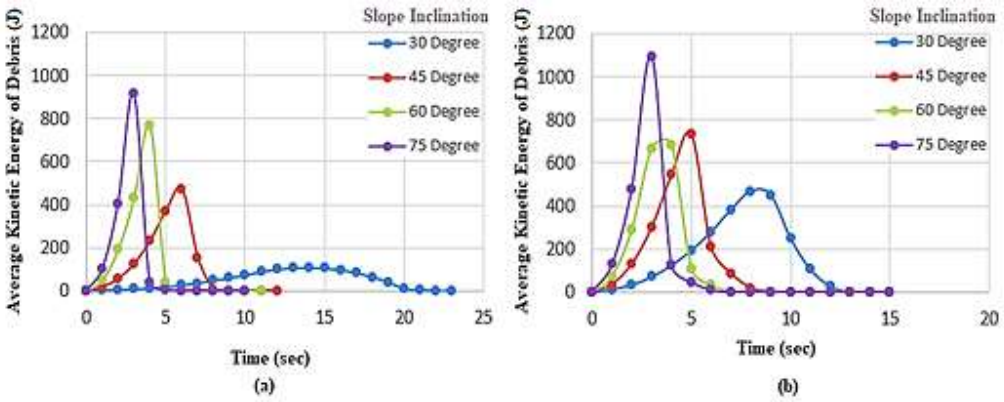

Fig. 7.19. Variation of the average kinetic energy of the flowing (a) Dry (b) Wet debris with time for different slope inclinations for a 40m high slope

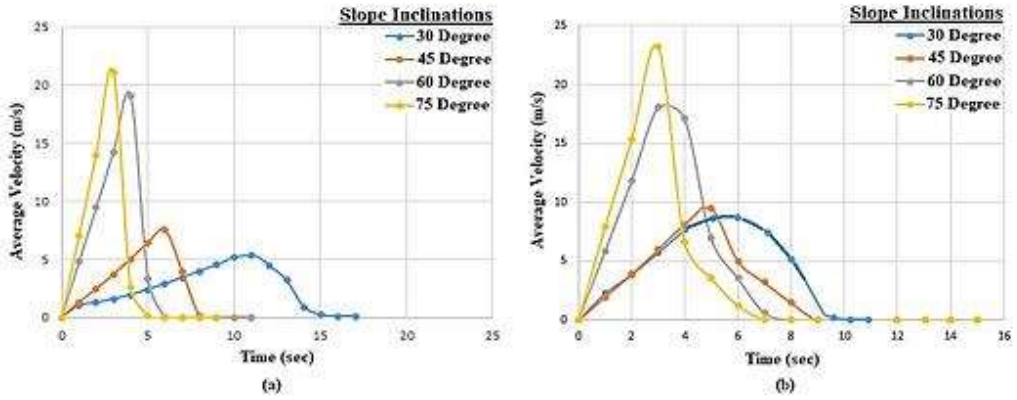

Fig. 7.20. Variation of the average velocity of the flowing (a) Dry (b) Wet debris with time for different slope inclinations for a 40m high slope

7.5.4 Effect of Slope Profile

Three slope models of 40m height and 45^0 slope inclinations have the same position of toe and crest, whereas different slope profile (concave, flat and convex) was created in PFC for each dry and wet condition. The magnitude of curvature for the concave and convex slope was 0.0097. The mean distance travel (X_{mean}) and the corresponding variance of the spread of the debris measured from the toe of the slope is given in Table 7.7. For a concave and flat surface, X_{mean} does not show a significant difference, though X_{mean} for the concave slope was slightly lesser than a flat surface under both dry and wet conditions. Similar behaviour was visible in the average kinetic energy of the debris, where the maximum kinetic energy achieved for the concave slope was slightly lesser than the flat slope. In contrast, in the convex slope, it was just about 80% and 60% of the flat slope under wet and dry conditions, respectively (Fig. 7.21).

Table 7.7: Spread of debris from toe for different slope profile

Slope Profile	Dry Debris		Wet Debris	
	X mean	Variance	X mean	Variance
Concave	8.84	9.03	17.05	4.22
Flat	9.94	8.43	18.23	0.11
Convex	5.71	3.76	7.37	1.57

The time for flow was also high in the case of the convex slope. Fig. 7.22 depicts the average flow speed for the debris in different slope profiles for both dry and wet conditions, and it is clear that in the case of the concave slope, particles attain higher speed initially due to a steep slope. In contrast, in the convex slope, they move relatively slow initially due to the flatter slope. In comparison, the speed of the flowing debris reduces in the latter half in the case of concave slope due to gentle profile, and in the case of the convex slope, the speed increases due to the steeper lower part of the slope. While the debris flowing in the flat profile maintain their speed. It can be deduced from Fig. 7.22 that the particles flowing in a convex slope profile attain high speed and energy when it reaches near the toe of the slope. However, due to abrupt change in flow direction at the toe, it loses most of its energy, and the spread gets contained near the toe, but the destruction potential grows up whereas, due to smooth transition of resultant flow direction in case of concave and flat slope profiles, the particles can reach longer distance in valley thus may cause destruction in a larger area. From Fig. 7.21 and Fig. 7.22, it could be concluded that the effect of slope profile on average kinetic energy and velocity of the flowing debris is more pronounced in the case of dry flow when compared with the wet flow.

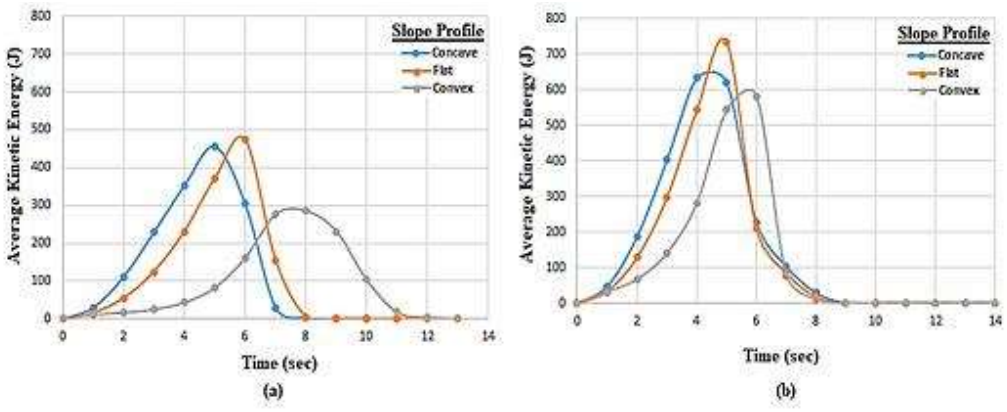

Fig. 7.21. Variation of the average kinetic energy of debris under (a) Dry and (b) Wet condition with time for a 40m high slope having different slope profile

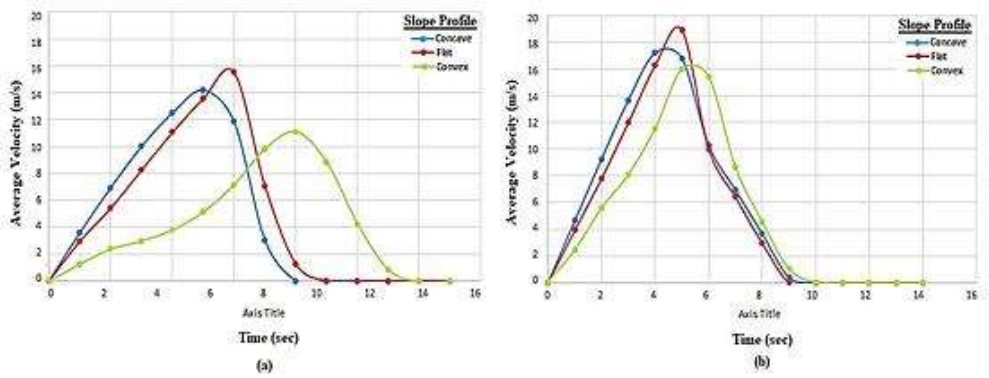

Fig. 7.22. Variation of the average velocity of debris under (a) Dry (b) Wet condition with time for a 40m high slope having different slope profile

7.5.5 Effect of Particle Size Distribution of Debris

Five models with a 40m slope height and an inclination of 45^0, having different gradation of the particles present in the debris, were created using PFC and analysed under dry and wet conditions. The size distribution and their fraction in the debris are shown in Table 7.8. With the increase in the fraction of larger boulders, randomness in behaviour also increases. The increased randomness is expressed in terms of the standard deviation (StD) of displacement from the toe (Table 7.9). It was observed that the randomness in the spreading of the debris is much more concentrated in the case of wet flowing debris when compared with the corresponding dry debris flow for a particular debris composition. With an increase in the fraction of larger boulders, it becomes hard to predict the damaged area. However, debris consisting of mainly finer particles show a much more concentrated spread than debris composed of mainly larger particles under both dry and wet flow conditions.

Table 7.8: Particle size distribution of the debris and their fraction for analysis of size effect

Size Range	1-50mm	50-200mm	200-500mm	500-1000mm
Only Fine	0.85	0.15	0	0
Mainly Fine	0.65	0.30	0.05	0
Normal	0.45	0.35	0.15	0.5
Mainly Bolder	0.20	0.30	0.35	0.15
Only Bolder	0	0.5	0.50	0.45

Table 7.9: Effect of particle gradation of debris on the distance travel by debris from toe

Debris Composition	Dry Flow			Wet Flow		
	Average Displacement from Toe (m)	StD of Average Displacement from Toe	Maximum Displacement from Toe (m)	Average Displacement from Toe (m)	StD of Average Displacement from Toe	Maximum Displacement from Toe (m)
Only Fine	4.91	1.87	17.7	16.71	0.1	21.22
Mainly Fine	6.93	1.98	22.3	17.83	0.31	27.21
Normal	9.32	2.73	28.6	18.87	1.58	37.46
Mainly Bolder	12.19	4.87	35.7	21.42	3.81	51.66
Only Bolder	17.89	7.96	46.8	25.21	5.92	64.79

The larger displacement of large particles can be attributed to the high inertia associated with large particles. Also, as observed in the previous analysis (Sections 7.5.1 to Section 7.5.4), the kinetic energy and velocity of coarser particles were high compared to finer ones in the debris mix. Fig. 7.23 shows the variation of the average kinetic energy of the flowing debris with different debris compositions under dry and wet flow. The average kinetic energy of particles in the case of only bolder debris is nearly 41 and 43 times higher than the average kinetic energy of particles in the case of only fine debris flowing under dry and wet conditions, respectively. The average flow velocity for different debris compositions is shown in Fig. 7.24.

A substantial increase in the average velocity of debris is observed with an increase in particle size under both dry and wet conditions. This high energy and high velocity give rise to a long and widely scattered flow of large particles. Thus, it can be concluded that an increase in the coarser fraction in the debris will increase the reach and non-uniform spread of the debris in the valley. Also, with the associated higher energy, it can prove to be much more catastrophic than debris containing a higher fraction of fine particles. Time taken by the debris to reach the peak velocity reduces with an increase in the particle size of the debris material. The peak velocity

attained by debris composed of only boulders is almost 7 times higher than debris composed of only fine particles, indicating the extreme damage potential of debris composed of only boulders.

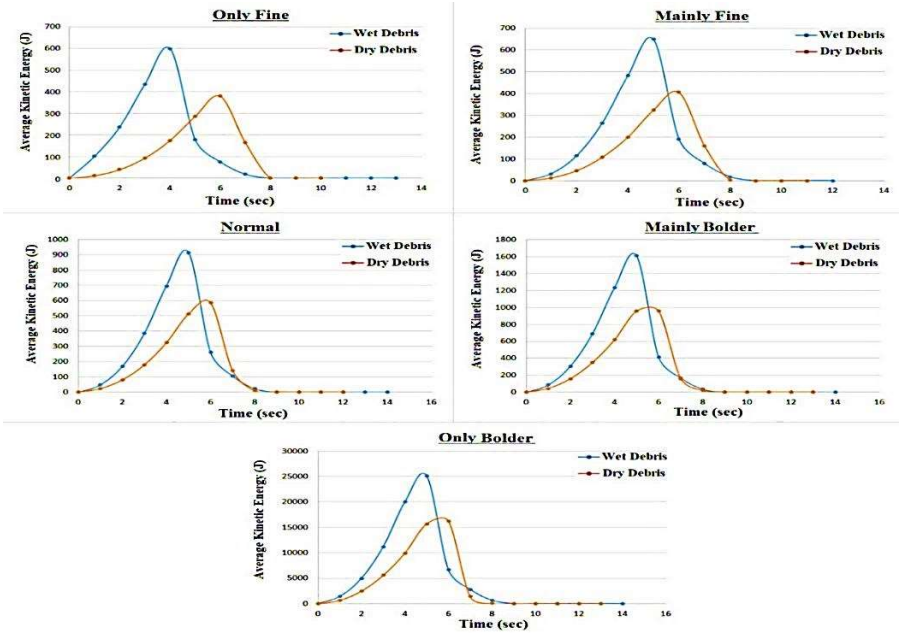

Fig. 7.23. The average kinetic energy with time for debris possessing different particle size compositions flowing over a 40m high slope with an inclination of 45^0

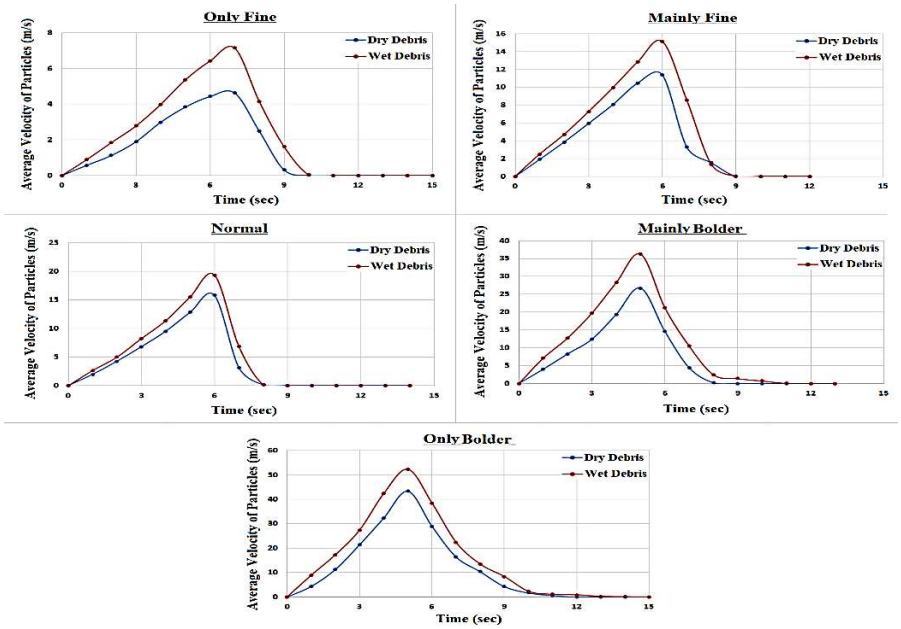

Fig. 7.24. The average velocity of flow with time for debris possessing different particle size compositions flowing over a 40m high slope with an inclination of 45^0

7.5.6 Effect of Retaining Wall or Debris Flow Barrier

Four models were created in PFC, having a 1.5m high rigid vertical retaining wall placed at different positions along the slope. The wall was positioned at the toe, 4m vertically from the toe, 8m vertically from the toe and 12m vertically from the toe, as shown in Fig. 7.25a. Constructing a wall at the upside (towards crown) will not serve the purpose as it will contain flow from a minimal area, and those materials which manage to topple over the wall will gain momentum while moving downslope. Thus, the study was focused on placing the wall in the bottom one-third of the slope.

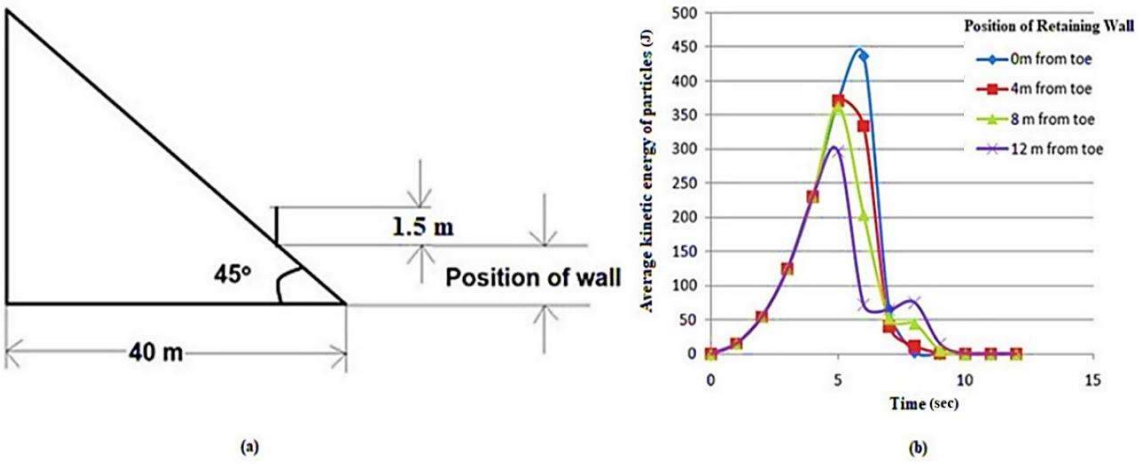

Fig. 7.25. Effect of retaining wall on flow of landslide debris (a) Position of the wall (b) Variation of the average kinetic energy of debris with time for different positions of the wall

Fig. 7.25b depicts the average kinetic energy attained with time for different positions of the wall. The traditional belief is that maximum kinetic energy is expected to exist at the toe, where almost all potential energy has been converted to kinetic energy. Placing a wall near the toe will be most practical since it can hinder debris flow. However, DEM analysis shows this may not be the case; instead, placing the wall slightly above the toe will prove beneficial. This observation was because when the wall is placed at the toe, the initial flowing debris starts filling up the backside of the wall and thus, a clear path is formed for the remaining flowing debris to move past

the wall without any restrain towards the horizontal direction (valley side). Thus, the effect of using a wall gets limited to just reducing the amount of free-flowing debris which gets retained by the wall. At the same time, the complete backfilled retaining wall acts as the new toe for the remaining flowing debris to move towards the horizontal direction.

When the wall is placed above the toe, the overflowing debris, instead of moving towards horizontal, move downwards due to gravity and starts rolling on the slope. This mechanism helps reduce the damage due to flowing debris in two ways. First, placing the wall a little higher than the toe does not allow the flowing debris to attain the peak velocity, as observed in the case of the wall placed at the toe (Fig. 7.25b). Second, the overtopped debris move along the remaining slope profile with lesser speed till it reaches the toe, as seen in Fig. 7.25b. The slope of the second peak, which represent the overtopped debris, is gentle compared to the peak for debris (no overtopping against retaining wall) flowing in case the wall is placed at the toe. Thus, it reduces the intensity of damage in the toe area. This is evident from various slope protection works using walls around the globe was observed to be placed above the toe. It is also evident that increasing the position of the wall more than a specific optimum value allows the particle to gain velocity again due to flow over the slope (Fig. 4.25b). So, the position of the wall should be optimised to keep the two peaks of kinetic energy (before and after impact) of the flowing debris minimum. This behaviour is also shown in Table 7.10 in terms of the displacement of particles that have overflowed the wall.

Table 7.10: Spread of the overflown debris from the wall calculated from the toe of the slope

Position of Retaining wall	**Mean Displacement from Toe (m)**	**Maximum displacement (m)**
0m from toe	5.17	30.83
4m from toe	1.84	26.27
8m from toe	2.96	29.65
12m from toe	4.47	31.04

Another important observation was that most of the debris was retained by the wall positioned at 4m above the toe of the slope for the current slope profile under investigation, as shown in Fig. 7.26a. However, the behaviour of different fractions of particles is not uniform, as shown in Fig. 7.26b. In every wall position, the maximum retainment was observed for finer particles, and this retainment decreases with an increase in the size of particles, with the least fraction being for large size boulders. Smaller particles (<200mm) show an almost similar trend as total particles (debris) as observed in Fig. 7.26a; however, larger particles (>200mm) show a slight increase in retention as the position of the wall moves closer towards the crown. This is because as the position of the wall moves upwards, the larger particles are unable to gain peak velocity while moving downslope; thus, some of the larger size boulders get retained. A detailed investigation of Fig. 7.26b also deduced that the utility of using the retaining wall as a mitigating structure would be most suitable in case the debris is made up of finer particles. In contrast, as the fraction of larger particles increases, its effectiveness decreases. Also, it can be deduced that the maximum utility of retaining wall in case of coarser debris will be achieved if it is placed at a higher elevation, while for finer debris, it must be placed nearby the toe.

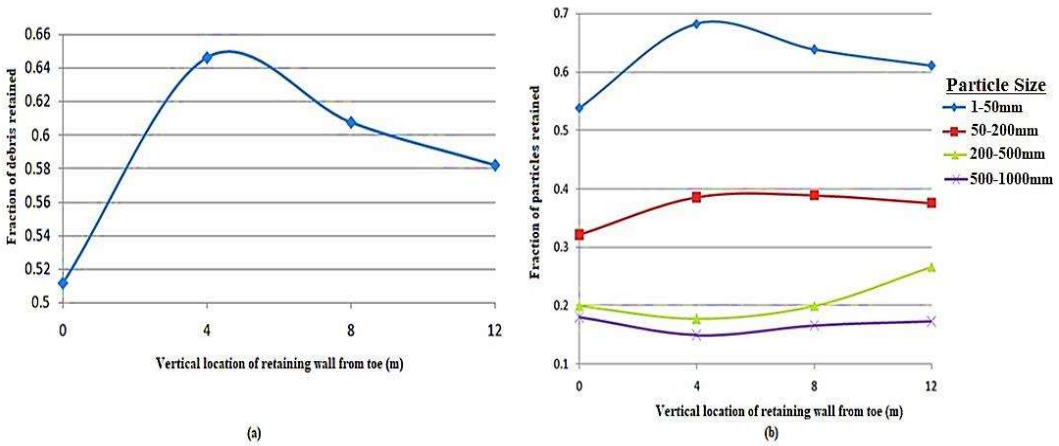

Fig. 7.26. (a) Fraction of overall debris retained by the rigid wall (b) Fraction of different sizes of particles retained by rigid wall placed at different positions along the slope

The stability of retaining wall/debris flow barrier is another important aspect that depends on many parameters, including rigidity of material from which the wall is made, i.e., concrete, brick, timber, wire mesh or stone masonry and the type of wall (rigid or flexible). Hence, the interaction of the flowing debris with the wall and after impact particle movement will depend entirely on the material type and its strength of the wall. However, the knowledge of the Force and Moment of Force distribution on a wall placed at a particular location on the slope surface will help in selecting and designing a particular wall type against debris flow. Thus, the variation of force (Fig. 7.27) and moment of force (Fig. 7.28) on the retaining wall were analysed, considering the wall as fully rigid and fixed.

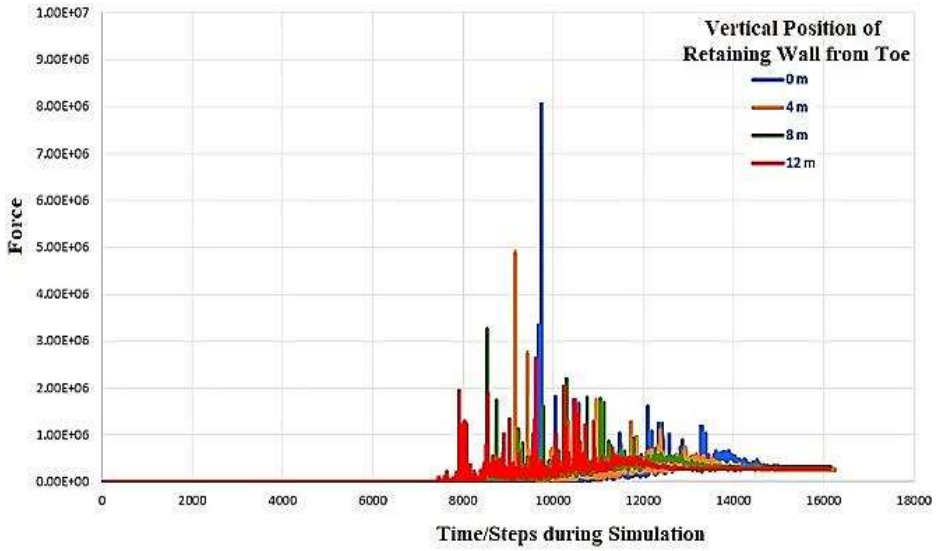

Fig. 7.27. Graphs depicting the variation of Force due to landslide debris on retaining walls positioned at different locations (in SI units)

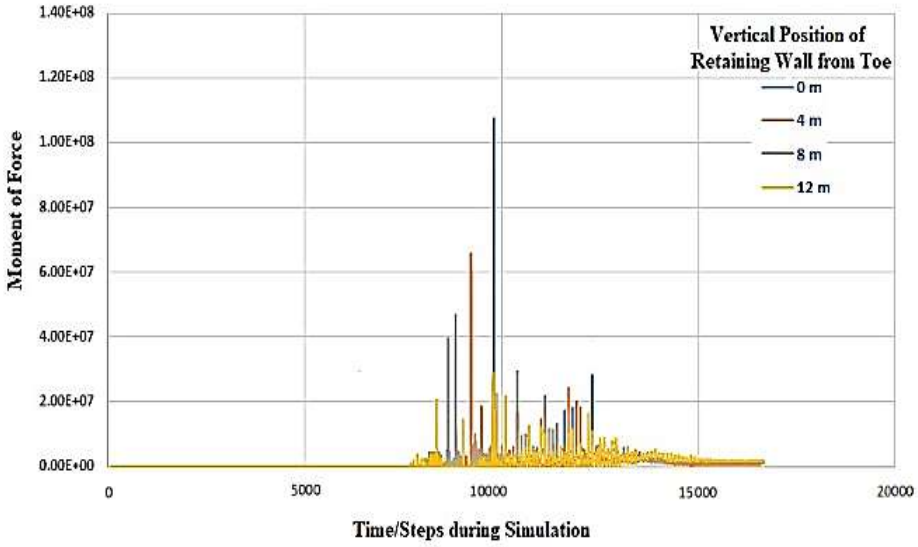

Fig. 7.28. Graphs depicting the Moment due to Force of landslide debris on retaining wall positioned at different locations (in SI units)

It is observed that the maximum impulsive force and moment of that force is acting when the wall is located at the toe of the slope. As the location of the wall is increased upslope, a continuous drastic reduction in maximum impulsive force and the moment is observed with the minimum at 12m height from the toe. This order is according to the average kinetic energy of the debris (Fig. 7.25b) striking the retaining wall at a different location. It was also observed that once the debris has overflown the wall and moved downslope, the force and moment on the wall does not return to zero as before the impact of the debris. This is due to the part of debris material that the wall has retained.

7.6 Discussion

Debris flow has caused severe human casualties and economic losses in landslide-prone areas. The study of the debris flow behaviour requires using a distinct element method. The methodology includes proper calibration of the developed numerical model using a physical model, followed by validation of the calibrated model. Calibration was performed by numerically

modelling the slope failure of a 60cm heigh residual soil slope made in the laboratory having an inclination of 45^0 and 50^0 and failure under both dry and wet conditions. The contact properties obtained from calibration was used to validate the Varunavat landslide debris flow. Properly calibrated and validated numerical model shows that very fine particles (<1mm) can be left out during simulation since they do not significantly affect the interparticle collision forces between the flowing debris, and choosing a very fine particle will unnecessarily increase the computational time. However, the smaller particles affect the contact properties during the flow, which was obtained during the calibration process and was later validated during the validation test. The contact properties obtained after the successful calibration and validation process was used for parametric analysis.

An apparent sorting phenomenon is observed within the debris particles during the accumulation process. Finer particles are widely distributed near the toe and bottom of the deposit, while the coarser particles are widely distributed in the front and surface of the deposit. Particle gradation significantly impacts the energy, speed, and distribution of debris deposits. The larger particles show more random behaviour, travel considerable distances, and possess higher energy. The presence of water allows the debris to reach a longer distance due to a reduction in damping during interparticle collision; however, the spread is observed to be more in the case of dry debris flow.

The maximum reach of debris in the horizontal direction depends on the combination of slope height, slope angle and water content. Increasing the slope angle, water content, and slope height will increase the energy and speed of the debris and eventually, the area affected by the slide will increase. With a five times increase in slope height (20m to 100m), there is almost 4 and 3.5 times increase in kinetic energy per unit volume in case of wet and dry debris, respectively.

The presence of water in the debris reduces the damping between inter-particle collision; thus, lesser dissipation of kinetic energy of the flowing debris takes place under wet conditions. A nearly perfect linear relationship is obtained for a mean distance (X_{mean}) travelled by entire debris from toe in the direction of valley and height of the slope. The X_{mean} in the case of wet debris is almost double compared to dry debris. However, for the individual size range of the debris, it was observed that with the increase in slope height, smaller particles show almost linear behaviour, whereas large particle shows a non-linearly trend.

Slope failure in the case of the gentle ($<40^0$) and steep ($>60^0$) slopes will result in more localised damages near the toe area in the valley whereas, failure in moderate (40^0-50^0) slopes will result in more widespread damage in the valley. The maximum displacement was observed in higher slopes with moderate slope inclination, specifically at a 45^0 slope angle. For all the cases of slope inclinations, the spread of debris under wet conditions is almost 2-3 times more than the corresponding debris under dry conditions. With an increase in slope inclination from gentle to steep (i.e., 30^0 to 75^0), the average velocity of the flowing debris increases by 2.8 to 4.4 times under wet and dry conditions, respectively and the average kinetic energy of the flowing debris increases by 2.5 to 9 times under wet and dry conditions respectively. However, overall, the kinetic energy and velocity of the wet debris are more than the dry debris for a particular slope angle.

The slope profile does affect the spread of debris. A flat and concave slope profile results in a more extensive spread of debris in the valley whereas, a convex slope profile results in a limited spread near the toe. The maximum kinetic energy and average speed of flowing debris show almost the same range in the case of concave and flat slope profiles. In contrast, flow in the convex slope, the maximum kinetic energy was just about 60-80% of the flow under flat slope whereas average speed is around 75%.

With the increase in the fraction of larger boulders in the debris, randomness in flow and settlement behaviour increases. Thus, it becomes hard to predict the damaged area. However, debris consisting of mainly finer particles show a much more concentrated spread under both dry and wet flow conditions. The standard deviation of average displacement from the toe indicates 4.25 times for only boulder debris compared to only fine debris under dry flow. Whereas it is 60 times under wet debris flow. With an increase in the fraction of larger boulders, it becomes hard to predict the damaged area. The average kinetic energy of particles in the case of only bolder debris is nearly 41 (dry flow) and 43 (wet flow) times higher than the case of only fine debris. The peak velocity attained by debris composed of only boulders is almost 7 (dry flow) and 7.5 (wet flow) times higher than debris composed of only fine particles. This indicates the extreme damage potential of debris composed of only boulders. The analysis indicates that the flow behavior of the debris are very complex and depend upon several topographical, geotechnical and hydrological parameters. Thus any developmental work in a landslide prone area must include debris flow analysis to limit the damage and destruction that may occure after a landslide.

The position of the retaining wall/debris flow barrier is vital to minimise the energy and flow of debris. The position needs to be optimised based on the energy gained by the flowing debris before hitting the wall and after overtopping the wall position. The fraction of particles in the debris is also a vital parameter in deciding the location of the retaining wall in the slope. The retaining wall was found to be suitable for retaining debris having finer particles. While the wall have failed to stop a sufficient quantity of debris composed of only boulders. The impact force due to flowing debris and the moment due to the force on the retaining wall is obtained for various wall locations on the slope. This will be beneficial while selecting and designing a particular type of retaining wall against debris flow.